Available online at www.sciencedirect.com

SCIENCE DIRECT®

Journal of Molecular Structure 754 (2005) 61–70

Journal of
MOLECULAR
STRUCTURE

www.elsevier.com/locate/molstruc

Density functional theory assessment of the thermal degradation of diclofenac and its calcium and iron complexes

Ihsan M. Kenawi*

Department of Chemistry, Faculty of Science, Cairo University, Giza, Egypt

Received 4 April 2005; revised 15 June 2005; accepted 17 June 2005
Available online 18 August 2005

Abstract

Thermogravimetric analyses of diclofenac sodium, its Ca^{2+} and Fe^{3+} complexes manifested a decreasing trend of the onset decomposition temperatures at which these compounds dissociated. The drop in the temperature was metal ion dependent; the sodium salt showed thermal stability up to 245 °C, whereas the complexes started their degradation processes at temperatures starting from 90 °C. While G* for the cleavage of the acetate moiety in the sodium salt was 63.76 $kJmol^{-1}$, it was 82.06 and 140.57 $kJmol^{-1}$ in the cases of Ca^{2+} and Fe^{3+}, respectively. However, their complete fusion took place at 187.65, 150.34 and 98.77 °C, respectively, displaying a reversed trend which is probably indicative of some catalytic part on the binding metals.

Using the *Gaussian 98 W* package of programs, *ab initio* molecular orbital treatments were applied to diclofenac and its Ca^{2+} and Fe^{3+} metal complexes to study their electronic structure at the atomic level. The thermochemistry of diclofenac sodium was followed through the TG fragmentation peak temperatures using the density functional theory calculations at the 6-31G(d) basis set level. The FT-IR data were in good agreement with the theoretically calculated values.

Single point calculations at the B3LYP/ 6-311G(d) level of theory, were used to compare the geometric features, energies and dipole moments of these compounds to detect the effect of the binding metal ions on the thermal dissociation of their diclofenac complexes.

Keywords: Thermal degradation; Density functional theory; Energy parameters; Dissociation constants; Diclofenac complexes

1. Introduction

Diclofenac sodium, monosodium {2-[(2,6-dichloroanilino) phenyl acetate, (dic), is germane as a mediator of the inflammatory processes. It possesses high promising value as a potential for inhibiting the conversion of arachidonic acid to prostalglandins. It is also a potent analgesic for painful attacks of non-rheumatic origin [1]. Due to its amino acid salt structure, dic is easily converted into salts of different metals and organic bases such as

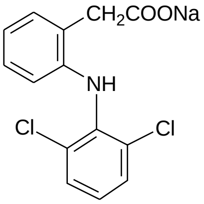

those prepared by O'Conner et al [2] including 2-amino-, 2-methyl-1,3-propanediol, 2-amino-2-methylpropanol, tert-butylamine, benzylamine and deanol. Diclofenac formed covalently linked compounds with acrylic type polymers (homopolymer of 2-hydroxyethyl methacrylate and its copolymers with acrylamide) to obtain macromolecule prodrugs [3]. It also has strong binding abilities forming coordinate bonds with some d-metal ions forming dinuclear macromolecules as Kovala-Demertzi et al. [4] reported.

Abbreviations dic, Diclofenac sodium.

* Corresponding author. Tel.: 20 263 53228; fax: 20 256 85799.
E-mail address: ihsanata77@hotmail.com.

0022-2860/$ - see front matter © 2005 Elsevier B.V. All rights reserved.
doi:10.1016/j.molstruc.2005.06.021

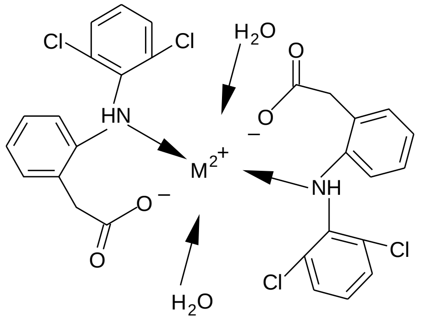

Scheme 1. Divalent metal complexes.

Kenawi et al. [5] prepared some s and d-metal complexes with diclofenac having the formulae Ca{(dic)$_2$.2H$_2$O}, Mg{(dic)$_2$.2H$_2$O}, Zn{(dic)$_2$.2H$_2$O} and Fe{dic}$_3$.3H$_2$O, according to Schemes 1 and 2.

Calcium and iron can cause metabolic disorders, which may be health hazardous, connected with both deficiencies and excessive amounts of these ions. Calcium deposits in bones and teeth; also in soft tissues. Iron normally functions as a protein hydrolysate chelate, which transports oxygen through the body. Thus, any instability in the content of either of these metal ions would result in grave disorders. The article [5] covering the synthesis of the calcium and iron complexes of divalent 2 s and trivalent 3d electrons lacked any information concerning the structural geometries or kinetic parameters. These data are an essential backup for the biomedical and pharmaceutical studies of such drugs; as complexes provide mechanisms for electron storage, for electron transport and for catalytic behaviour. A study of the thermal stability of these complexes would help in the design of new chemical profiles for the diclofenac binding sites. The TG parameters characterize the stepwise pyrolysis of these compounds, thus throwing more light on their structure formed through several-stepped mechanisms where the temperature range for each step may overlap, leading to irregular mass-temperature curves that can be difficult to analyze via practical methods. The change in the values of these parameters on complex formation is traced through mathematical calculations using the Coats–Redfern program [6]. The activation energies, E*, S*, G*, the activation enthalpy, H*, as well as the specific reaction rate, k$_r$, and dissociation equilibrium constant, K$_s$, for each step, were calculated. The Arrhenius equation [7] was used to calculate the reaction rates.

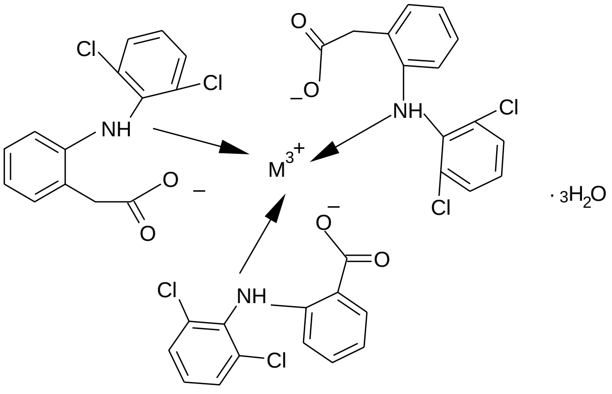

Scheme 2. Fe complex.

Some theoretical progress was made to cover the optimal set and geometry of the above mentioned adducts. By applying the *Gaussian 98 W* package of programs [8], the density functional theory was used to implement and provide new insights into their chemical behaviour through a systematic study of the electronic structure and bonding characteristics, comparing the energy quantities and dipole moments of dic and its calcium and iron complexes. This was done using the B3LYP level of theory at the 6-311G(d) basis set. To give a comprehensive view of the reaction mechanism resulting by fragmentation through the degradation process, a theoretical follow up of the thermochemistry of dic was calculated at the dissociation peak temperatures using the same theoretical method at the 6-31G(d) basis set level. The resulting frequencies were compared with the experimental values obtained by FT-IR studies to assess the applicability of the calculations, and to detect the presence of imaginary frequencies.

2. Experimental

Thermogravimetric analyses were run on Shimadzu TGA-50H in a nitrogen atmosphere with a rate flow of ($\theta = 20$ ml/min) and (10 °C/min) using from 3 to 6 mg test samples and heating up to 800 °C. Differential analyses were run on a Shimadzu DTA-50 H in nitrogen atmosphere at a rate flow 15 ml/min with 10 °C/min up to 1000 °C. The thermally inert reference material used was α-Al$_2$O$_3$ (Shimadzu Corp.). A HANNA H18417 *p*H meter was used to adjust the pH of the drugs with concentrated carbonate-free NaOH. IR spectra were recorded on a Pye-Unicam SP3-300 (500–4000 cm^{-1}) and a MATTSON 5000 FT IR (200–800 cm^{-1}) spectrometers. A Magnetic Substance Balance, Sherwood Scientific, Cambridge Science Park; Cambridge, England (sample tube length 1.5 cm) was used to detect the magnetic susceptibility of the ferric complex. All chemicals used were analytical grade and water was twice distilled.

2.1. Metal chelates

The complexes were prepared by mixing 100 ml of (0.01 M) calcium nitrate and ferric chloride with 200 and 300 ml, respectively, of 0.01 M aqueous solutions of dic and the *p*H was adjusted to ~6.5, stirring the precipitate for 6 h. The formed precipitate was filtered, washed and dried under vacuum, thus, being ready for elemental, thermal analyses and IR spectroscopy.

2.2. Methods of calculations

2.2.1. Integral method

The energy parameters resulting from the thermal analyses were calculated using the Coats–Redfern equation [6]. The energy of activation, (E^*), was calculated from the proposed integral equation:

$$\log\left[\ln\left(Wf/Wf-Wt\right)/T^2\right]$$

$$=\log\left[AR/\phi E^*\left(1-2RT/E^*\right)\right]-E^*/2.303RT\div$$

Since the whole logarithmic term is practically constant for the temperature range over which all the reactions generally occur, therefore

$$\log\left[\ln\left(Wf/Wf-Wt\right)/T^2\right]=\log\left(AR/\phi E^*\right)-E^*/2.303RT\div$$

Where A = Arrhenius constant; Wf = mass loss at completion of the reaction; Wt = mass loss up to temperature T (K); $Wf-Wt$ = mass remaining at T (K); T = absolute temperature K; R = gas constant; E^* = activation energy in J mole^{-1}; ϕ = heating rate, deg. min^{-1}.

A plot of the left hand side against $1/T$ would give a straight line from whose slope E^* may be calculated; and form whose intercept the Arrhenius constant is calculated. The activation entropy, S*, the activation enthalpy, H*, the free energy of activation, G*, and the specific rate, k_r, and stability, K_s, constants were calculated concurrently, from the following equations:

$$S^* = 2.303\log Ah/kTR$$

$$H^* = E^* - RT$$

$$G^* = H^* - T_S S^*$$

$$k_r = A\exp^{-E*/RT_S}$$

$$\Delta G = -RT\ln K_S$$

2.2.2. Computational methods used

The computer used in the theoretical studies was a CPU: AMD ATHLON XP 1.8 GHz, RAM: 256 DDR/333 MHz; CACHE: 512 K; GRAPHIC PROC.: RADEON ATI7200 64 DDR mb.

The computations of single-point refinements, geometric parameters, vibrational frequencies and activation energies were carried out at the Density Functional level of theory (DFT) using the *Gaussian 98 W* package of programs [8]. The DFT methods compute electron correlation via general functionals of the electron density. These partition the electronic energy into several components, which are computed separately; the kinetic energy, the electron-nuclear interaction, the coulomb repulsion and an exchange-correlation term accounting for the remainder of the electron-electron interaction [9]. The gradient corrected functionals involve both the values of the electron spin densities and their gradients. Single-point refinements of dic and its complexes were carried out at the B3LYP/6-311G(d) level of theory on the fully optimized geometries. The B3LYP is the keyword for the hybrid functional, [10], which is a linear combination of the gradient functionals proposed by Becke [11] and Lee, Yang and Parr [12], together with the Hartree–Fock local exchange function [13].

Most ferric ion complexes [14] are in the high spin state $\left(t_{2g}, e_g\right)$, but those subjected to a strong field ligand are in the low spin state $\left(t_{2g}\right)$. To write the correct molecule specification (spin multiplicity) of the iron complex, magnetic susceptibility of the solid complex was studied and the multiplicity was found to be 2. This agrees with our previous uv spectroscopic studies [15] that showed the presence of charge transfer in dic. The frequency vibrations and activation energies, at STP and at the TG dissociation peak temperatures, were calculated at the B3LYP/6-31G(d) level of theory, after being fully optimized.

3. Results and discussion

Elemental analysis showed the Ca^{2+} and Fe^{3+} complexes of dic to be 1:2 and 1:3 M:L, respectively

3.1. Thermal processes

The thermograms of dic and its calcium and iron complexes, Fig. 1, traced the weight loss steps into four distinct changes, always losing water molecules in their first mass loss step, thus agreeing with Fini et al. [16]. The results in Table 1 are reported in terms of mass loss percent with the coinciding temperature ranges of the TG peak decomposition temperatures and DTA peak temperatures. The cleaved groups and the remaining moieties are calculated

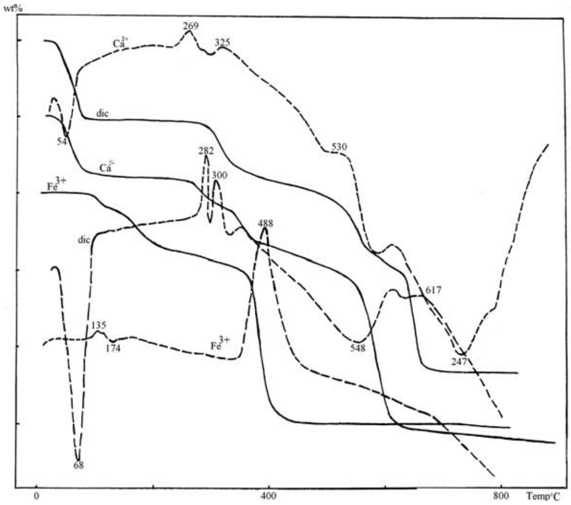

Fig. 1. TG(–) and DTA (––) thermograms of dic and its complexes.

Table 1
Thermodynamic functions of dic and its calcium and iron complexes

Sample	Temp. range °C	% mass loss	Lost groups	DTA peaks K	Peak
Dic	20–95	19.9	$4H_2O$	68.44	Endothermic
	248–395	15.1	CH_2COO	282	Exothermic
				300	Exothermic
	397–570	19.4	Phenyl	548	Endothermic
	570–647	29.6	Phen.NHCl	617	Exothermic
Residue		15.2	NaCl		
Dic_2Ca	21–132	15.9	$2H_2O,CO_2,O$	54	Endothermic
	136–299	7.7	$2CH_2,CO$	269	Exothermic
	300–420	13.1	Phen.NH	325	Exothermic
	420–664	48.4	3Phen,NH,2Cl	747	Endothermic
Residue		14.8	$CaCl_2$		
Dic_3Fe	Stable to 92 $3H_2O$				
	92–153	5.6	2CO	135	Exothermic
	160–323	13.8	$3CH_2,CO_2,O_2$	174	Endothermic
	325–400	4.0	3NH	355	Exothermic
	410–670	61.7	6Phenyl, 3Cl	488	Exothermic
Residue		16.4	$FeCl_3$		

and therein depicted. Agreement with the experimental values was within the range of 0.25 to 1.8%. An important observation was drawn from these results; which is that the thermal dissociation of these compounds took place according to a, more or less, regular pattern. The acetate moiety was the first to go, yet more readily so from its attachment in the cases of the complexes, where the enthalpy change commenced at a lower onset temperature; almost 100 °C less than in the case of the sodium salt. Meanwhile, the acetate groups present in the Ca^{2+} and Fe^{3+} complexes were not completely dissociated until the second mass loss step. On the other hand, the rupture of the phenyl ring from the remaining dichloro–diphenylamine moieties occurred at very close onset temperatures in the two complexes, but at ~100 °C less than the salt. The final fusion resulted in all three cases in a metallic chloride residue. The onset temperatures were almost equal in the complexes but 150 °C less in the sodium salt. The results that were confirmed by DTA, showed that coordination caused steric constraints that weakened the bonds. A fact that agrees well with their consecutive melting points (283–5 Na, 250–1 Ca and 150 °C for Fe) that are previously reported [5]. It would then be appropriate to assume that thermal stability is affected by the metal ion type involved in binding, to the order of Na > Ca > Fe.

Thus, thermal dissociation might probably follow a somewhat similar trend as in Scheme 3, after the loss of water.

In an attempt to further, understand such a dissociation mechanism, an investigation of the kinetic pyrolysis parameters was carried out, utilizing the mathematical algorithms introduced by Coats–Redfern [6] and Arrhenius [7]. The activation energies and the stability and specific rate constants are all depicted in Table 2 The correlation coefficient, R^2, that evaluates the accuracy of the calculations, is also reported.

These reactions may be considered bimolecular nucleophilic addition reaction, as seen from this data [17].

The activation energy, E*, necessary to cleave the acetate group from the parent compounds was a positive quantity that increased remarkably (as shown in Scheme 4) in the case of the complexes; being 56.58, 84.76 and 149.11 $kJmol^{-1}$ for Na^+, Ca^{2+} and Fe^{3+}, respectively.

The acetate detachment, in the complexes, was completed in the second mass loss step; having values of E* 64.19 and 38.21 $kJmol^{-1}$ for calcium and iron, respectively. Thus, the order of activation energy required would be $E_{Fe} > E_{Ca} > E_{Na}$. This relates to the ionization potential values of these metal ions, namely, 5.14, 11.87 and 30.64 eV for Na^+, Ca^{2+} and Fe^{3+}, respectively [14]. However, E* required for the completion of the third and final mass loss steps, in which the amine completely dissociates, manifested a reversed trend where $E_{Na} > E_{Ca} > E_{Fe}$ having the values 127.07and188.92 for Na^+, 62.96 and 148.87 for Ca^{2+} and 18.84 and 91.63 $kJmol^{-1}$ for Fe^{3+}. This is in agreement with the melting points of these compounds. The above mentioned results point to the weakening of the London forces [18] due to complex formation.

Another point of importance is the very large drop in E_{Fe} starting from the second loss step where the metal ion was broken from the complex. This value may be ascribed to some catalytic behaviour on part of the iron.

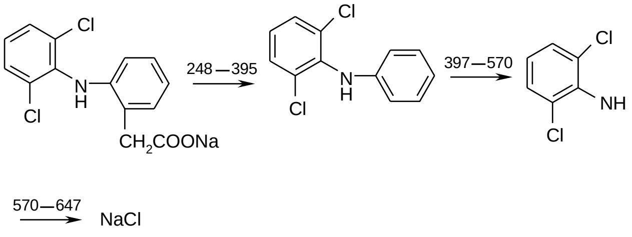

Scheme 3.

Table 2
Energy parameters of the thermal degradation of dic and its Ca^{2+} and Fe^{3+} complexes

Adduct	Step	R^2	T_s K	E*	S*	H*	G*	k_r m^{-1}	K_s
Dic	1	0.999	332	62.54	−8.59	59.78	62.63	1.91E-01	1.42E-10
	2	0.997	586	56.58	−20.56	51.70	63.76	1.34E-01	2.11E-06
	3	0.993	803	127.07	−13.14	120.39	130.94	1.83E-01	3.09E-09
	4	0.993	901	188.92	−6.91	181.42	187.65	2.11E-01	1.33E-11
Dic_2Ca	1	0.999	333	84.76	−0.22	81.98	82.06	3.00E-01	1.42E-13
	2	0.994	540	64.19	−17.29	59.69	69.03	2.22E-01	2.14E-07
	3	0.994	602	62.96	−19.44	57.94	69.65	1.60E-01	9.18E-07
	4	0.997	807	148.87	−10.15	142.15	150.34	1.55E-01	1.87E-10
Dic_3Fe	1	0.991	415	149.11	12.26	145.66	140.57	3.22E-01	2.08E-18
	2	0.996	500	38.21	−23.56	34.05	45.83	0.63E-01	1.64E-05
	3	1.000	637	18.84	−20.23	13.54	26.42	0.63E-01	6.82E-03
	4	0.993	751	91.63	−17.84	85.39	98.77	1.20E-01	1.35E-07

E*,H*,G* in $kJmol^{-1}$; S* in $JKmol^{-1}$.

The values of the entropy of activation, S*, of all three compounds are negative numbers that are average in value, thus the reaction rate would be also of moderate value; neither faster nor slower than predicted by the collision theory [19]. The presence of the methyl group, in the ortho position, exerts both inductive and steric effects. These cause an increase of the negative charge on the nitrogen atom, which result in the lowering of entropy values [17]. Thus S* should increase once the acetate group is dissociated. The only positive S* value of the activation entropy is that of the first mass loss step in the iron complex, which is 12.26 $JK^{-1}mol^{-1}$, indicating an irreversible change where the two CO lost have different ranges of rotational and vibrational levels open to them. There also exists a high probability of an increase in the rate of reaction due to a catalytic behaviour of the ferric ions.

S* for the complete release of the acetate group has close values in all three, being −20.56, −17.29 and −23.56 $JK^{-1}mol^{-1}$, for Na^+, Ca^{2+} and Fe^{3+}, respectively. Yet, the release of the CO, CO_2 and O in the first mass loss steps in calcium and iron, possess a much larger value of entropy, −0.22 and 12.26 $JK^{-1}mol^{-1}$, probably due to some catalytic behaviour of these metal ions which increase the entropy by increasing the rate of reaction. In the sodium salt, contrary to the expected, there was a large drop of S* (−8.59 to −20.56) as the temperature was raised. This is due to the loss of water of hydration which is easily vaporized and the remaining molecules possessing smaller entropy values, as they are solids and thus do not move as freely. On increasing the temperature, the entropy follows the regular trend in increasing gradually until it reaches its peak value (−6.91 $JK^{-1}mol^{-1}$) at the final step of losing all the phenyl rings.

After the first step, the complexes show a similar trend of decreasing entropy, which may be attributed to the existence of a steric factor as a result of the large size of the existing groups causing hindrance to the course of the formation of complexions and thus decrease in S*. Once these groups break away, the entropy follows its general course of increasing with temperature.

The activation enthalpies, H*, or the heats of atomization, of the thermal dissociation of these compounds were calculated to be positive values, thus indicating endothermic reactions that need energy to break the existing molecular bonds. In the sodium salt, the loss of water required 59.78 $kJmol^{-1}$; this was decreased to 51.70 $kJmol^{-1}$ for the acetate fission. This is again much less in the case of the break away of this group in the complexes, where it took place along two loss steps with H* being equal to 81.98 and 59.69 $kJmol^{-1}$for calcium; and 145.66 and 34.05 $kJmol^{-1}$ for iron. The doubled and tripled amounts of enthalpy are probably due to the presence of more bonds to break due to the existence of two and three acetate groups attached to the metal ions in the complexes. The methyl group, in the *o-position* to nitrogen, exerts both inductive and steric effects. The inductive effect increases the effective negative charge on the nitrogen atom, in other words nucleophility increases [17]. Therefore, H*, is higher after the acetate group cleavage. The loss of one phenyl group in dic needed double that amount (120.39 $kJmol^{-1}$), while the final fusion of the salt with NaCl remaining as residue, used up 181.42 $kJmol^{-1}$. This is much less than the bond enthalpy of a chlorine molecule (+242 $kJmol^{-1}$), and ΔH° of NaCl (−411.15 $kJmol^{-1}$) [19].

Meanwhile, the sudden decrease in the value of H*, in the second and third loss steps of the iron complex

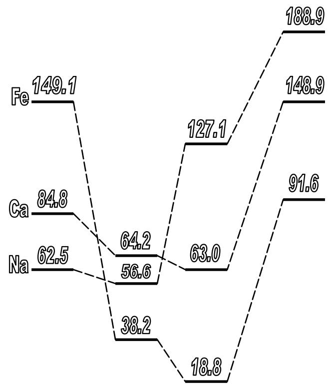

Scheme 4.

(34.05 and 13.54 $kJmol^{-1}$), points out its catalytic behaviour.In the case of Ca^{2+}, a slight decrease in H* is also noticed at the third mass loss step (57.94 $kJmol^{-1}$). This may be explained as a degree of instability caused by steric constraints. However, the final fusion requires three folds the amount (142.15 $kJmol^{-1}$); probably caused by the formation of the ionic $CaCl_2$ residue; a value incomparable to ΔH° of both Cl_2 and $CaCl_2$ (−795.8 $kJmol^{-1}$) [19]. On the other hand, the final fusion of the iron complex exceeds, by six fold, the preceding enthalpy value (85.39 $kJmol^{-1}$).

The positive values of the free energies of activation, G*, calculated from the thermograms, indicate that these dissociation processes are non-spontaneous reactions that do not do work and are not thermodynamically favoured. They are endergonic processes obtaining their energy content from the gradually raised temperature. Though these values showed, in the case of dic, a somewhat regular increasing trend accompanying temperature increase, the pattern changed in the cases of the complexes. The loss of the four water molecules of hydration of dic contained 62.63 $kJmol^{-1}$, which is far more than the reported (−220.6) standard free energy of formation of $H_2O_{(g)}$ [20]. The loss of the acetate group had a G* value of 63.76 $kJmol^{-1}$, which is almost equal to that of the loss of water, and that is due to the corresponding very low value of S* (−20.56J $K^{-1}mol^{-1}$), even though the temperature was 586 K. The value of G* was doubled (130.94 $kJmol^{-1}$) on the loss of one phenyl group and went further up to 187.65 $kJmol^{-1}$ for the final fusion of the compound yielding NaCl. This is so much higher than the reported value (−384.14 $kJmol^{-1}$) for ΔG° of the formation of solid NaCl [19]; thus confirming the endergonic character of the process. Meanwhile, the decrease of the values of G* in the complexes was noticed. The first mass loss step (82.06 and 140.57 $kJmol^{-1}$ for Ca^{2+} and Fe^{3+}, respectively) suddenly dropped in the case of iron to 45.83 $kJmol^{-1}$. This is a result of its catalytic character, which lowered the saddle point of its energies of activation. The second and third mass loss steps in the calcium complex were almost equal (69.03 and 69.65 $kJmol^{-1}$) and almost half that of the corresponding loss step in dic, probably due to the presence of two diclofenac groups in the complex. The third loss step in the iron complex had a G* value of 26.42 $kJmol^{-1}$, half the amount of the previous step that completed the acetate group cleavage. This, again, may be ascribed to the catalytic character of Fe^{3+}, being activated by its breaking loose. In the final step in both complexes, G* increased again as dissociation was completed.

These pyrolysis results show that the energies of dic are cation dependant on the s and d orbital metals studied in this work. Complex formation resulted in a change in some physical properties, as well as steric constraints that must be operative to give energy-preferred orientation of the system resulting in stronger binding free energy.

The specific reaction rates, k_r, were all of the order 10^{-1}, showing slight differences between the mass loss steps for each compound; except in the case of iron, where the complete loss of the acetate and the three NH groups are 10 fold faster than all other loss steps being 0.632×10^{-1} and 0.627×10^{-1} min^{-1}, respectively. It then decreases back to 1.2×10^{-1} min^{-1}; due to the catalytic behaviour of the Fe^{3+} ions. Generally, these dissociation processes are of moderate rate, a fact that agrees with the not very large negative number of the entropy values of these reactions [19]. The cation type slowed down the rate slightly from sodium to calcium, but the catalytic abilities of iron somewhat counteracted this effect, thus; $k_{Fe}>k_{Na}>k_{Ca}$. The dissociation equilibrium constants, K_s, of the TG mass loss steps of dic and its complexes, ranged in the order of 10^{-3} up to 10^{-18}. According to Le Chatelier's principal, the increase of temperature favours the products of an endothermic reaction. The resulting K_s values increased as the thermal dissociation proceeded, but increased once more as the final fusion processed. By comparing K_s for each step in all three compounds, it appears that the calcium complex reached equilibrium at a slower rate than the sodium salt; and was less stable as a result of the binding with NH which probably caused steric constraints. The equilibrium constant of Ca^{2+} was 2.14×10^{-7} and that of dic was 2.11×10^{-6}.

The Fe^{3+} complex, on the other hand, exerted a catalytic effect and reached equilibrium quickly with a much higher K_s value of 1.65×10^{-5}. Naturally, a catalyst will increase both the forward and reverse rate processes so that a reaction will reach equilibrium sooner. This is quite apparent in the third loss step where K_s is 6.82×10^{-3} for Fe^{3+}, while it is 3.09×10^{-9} and 9.18×10^{-7} for Na^+ and Ca^{2+}, respectively. Stability of the complexes is reached quicker and the products are more stable due to the higher values of electronegativity of these metal ions (Na 0.9, Ca 1.0, Fe 1.8) [18]. The formed $CaCl_2$ and $FeCl_3$ consequently form stronger ionic bonds than NaCl; K_s being 1.87×10^{-10}, 1.35×10^{-7} and 1.33×10^{-11}, respectively.

The amount of reactants at the dissociation peak temperatures were 32.05, 39.99 and 51.86% for dic, calcium and iron complexes. This means that the iron complex was the one that was least thermally stable, followed by the calcium complex and the sodium salt was the most stable of all three. Thus, it may be concluded that the replacement of the Na^+ ion by these metals caused steric hindrance due to coordination that affected the thermal stability of the drug, which is confirmed by the lowering of the respective melting points.

3.2. Theoretical simulations

3.2.1. Thermochemistry of dic fragments

The thermochemistry of dic and its fragments that resulted during the thermal dissociation were studied theoretically using the density functional theory, applying the B3LYP/6-31G(d) level of theory. By default, analysis is carried out at 298.15 K and 1 atmosphere of pressure using the principle isotope for each element type [21]. However,

Table 3
Thermal energies predicted at the B3LYP / 6-31G(d) level of theory

Loss step fragments	SCF,au (STP)	ΔE,au (T_S K)	ΔE,kJ	ΔH, au (T_s K)	ΔH,kJ
$T_s=586$ K					
Dic	1579.631496	0.198513	522.93	0.199105	521.96
$Cl_2\Phi NH\Phi$	1268.745554	0.169251	445.85	0.170084	445.90
CH_3COONa	344.876663	0.049348	129.99	0.050181	131.55
$\Delta E^*=52.91$ kJmol^{-1}				$\Delta H^*=55.47$ kJmol^{-1}	
$T_s=803$ K					
$Cl_2\Phi NH\Phi$	1268.745554	0.169998	447.82	0.170111	448.11
$Cl_2\Phi NH_2$	1064.874363	0.108631	286.16	0.109111	286.05
Φ	204.936088	0.108856	286.75	0.108421	284.24
$\Delta E^*=125.07$ kJmol^{-1}				$\Delta H^*=122.18$ kJmol^{-1}	

by specifying the READISOTOPE option to the FREQ keyword in the route section, it was possible to study the thermochemistry of these reactions at the specified peak temperatures, T_s.

The difference, ΔE, for the two intermediate dissociation reactions whose energies were computed at STP and the consecutive T_s temperatures, was taken as an equivocal value of the amount of activation energy, E*, that would be required to complete such reactions. A slight deviation from the experimental values might be because of the choice of the medium sized basis set 6-31G (d). The choice of such a size of basis set was because higher sets may lose the negative frequency values that indicate a saddle point of energy. This imaginary frequency is due to the presence of an intermediate complexion that takes part in the reaction. However, one may reliably compare the computed values to the experimental ones since these results, Table 3, are much closer than expected. The change in the energies, as dissociation processes, followed a similar trend to the experimentally calculated parameters. That is, cleavage of the acetate group was computed to have $\Delta E^*=53$ kJmol^{-1} and $\Delta H^*=55$ kJmol^{-1}, whereas the experimental values were 56 kJmol^{-1} and 52 kJmol^{-1}, respectively. The loss of one phenyl ring from the dichloro diphenylamine was computed at $\Delta E^*=125$ kJmol^{-1} and $\Delta H^*=122$ kJmol^{-1}, whereas the experimental values were 127 kJmol^{-1} and 120 kJmol^{-1}.

As the calculation of such complicated systems becomes more complex, the theories must still be tested. Thus, a comparison of the experimental ir frequencies of dic with the computed values is important. The results, Table 4, were in good agreement. In the simulated frequencies, there appeared four negative values, thus confirming the presence of an intermediate complexion involved in the procession of the thermal dissociation of dic.

3.2.2. Electronic structural modeling.

The substitution in dic of the sodium ion by either calcium or ferric ions, or in other words the formation of coordinated adducts, resulted in steric constraints that initiated a change in geometry to give an energy preferred orientation. Thus, the molecular energies and structures of dic and its calcium complex were simulated through single point energy calculations at the B3LYP level of theory with a 6-311G (d) basis set after being fully optimized. This high basis set has been chosen to detect the dipole moments at a very accurate level. The first optimization step of the complexes was carried out on the Hyperchem 6 package using ZINDO 1 semi-empirical methods. To obtain a higher level of optimization these structures were run on the *Gaussian98 W* package. The sodium salt was optimized using the B3LYP level with a basis set of 6-31G (d). The calcium complex was a difficult optimization case, thus the approximate matrix was improved through use of the computed first derivatives obtained from the STO-3G size basis set. The iron complex would not be optimized as convergence would not be met, an error message repeatedly appearing at the L502 link. Thus, a comparison of its dipole moment with the other compounds was restricted to the ZINDO1 level of theory.

The increasing electronegativity [18] of the substituted metals will cause the carbon in the COO^-group to supply more p orbital character which results in distortion, of the geometric parameters, from the ideal values. The output standard orientation of the optimized structures of all three

Table 4
FT-IR and theoretically calculated frequencies, cm^{-1}, at 6-31G(d) level, for dic and its complexes

Assignments	Experimental	Theoretical
Ring stretch	417	418
	459	460
	513	516
	548	545
	683	687
	718	720
γCH–Cl	760	759
γCH	869	867
δCH	1161	1162
νC–N	1292	1290
$\delta_s COO^-$	1409	1405
ν_M	1454	1454
δCH_2COO^-	1472	1471
δNH	1625	1622
νCH_2	2968	2963
νNH	3422	3429

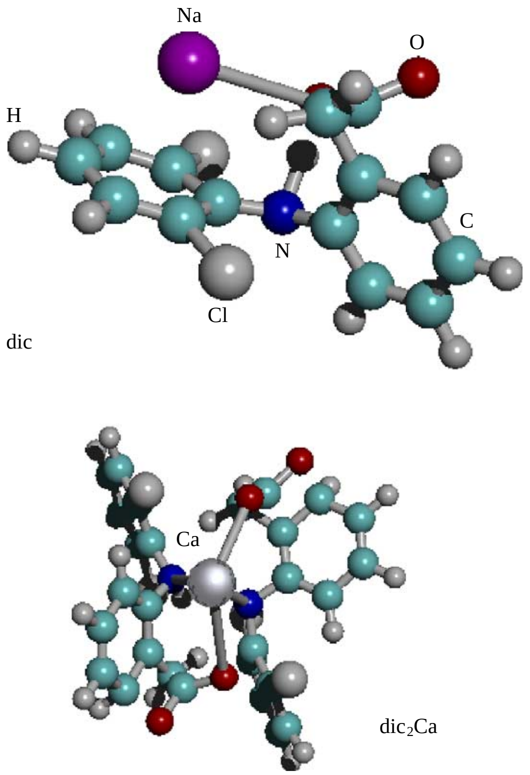

Fig. 2. Optimized structures of dic and its calcium complex.

Table 5
Bond angles, order and lengths of dic and its complexes computed at the B3LYP/6-311G(d) level

Atom no.	Na^+	Ca^{2+}	Fe^{3+}
Bond angles, in degree			
O2 C3 O4	114.998	121.059	117.108
O2 C3 C5	122.606	127.340	123.702
C5 C6 C7	127.391	128.458	130.795
C6 C7 N8	125.203	112.630	116.013
C7 N8 C9	124.799	117.134	110.280
N8 C9 C11	128.260	120.428	116.663
C9 C10 Cl12	116.675	120.947	115.690
Bond order			
M1–O2	0.100	0.616	0.186
C6–C5	0.917	0.992	1.018
C5–C3	0.954	0.983	0.967
C3–O4	1.381	1.617	1.688
C3–O2	1.155	1.212	0.950
C7–N8	1.101	0.947	0.985
N8–C9	1.102	1.032	0.991
C11–Cl13	0.863	0.862	0.852
C10–Cl12	0.831	0.862	0.863
N8–M1	–	0.179	0.339
Bond length, in Angstrom			
M1–O2	3.211	2.541	2.451
C6–C5	1.514	1.514	1.485
C5–C3	1.492	1.514	1.483
C3–O4	1.308	1.451	1.294
C3–O2	1.363	1.411	1.383
C7–N8	1.405	1.456	1.427
N8–C9	1.371	1.446	1.462
C11–Cl13	1.741	1.777	1.735
C10–Cl12	1.743	1.779	1.745
N8–M1	–	2.445	2.264

compounds, Fig. 2, shows all the atoms to be occupying the x, y and z planes with the two phenyl rings of the dichloro–diphenyl amine at a dihedral angle of ~108°. Thus, the cations did not affect the torsion angles of these two rings. However, some bond angles (Table 5) varied in their values due to steric constraints resulting on complex formation and consequently, a slightly different hybridization. The angles O2-C3-O4, C5-C3-O2 and C5-C6-C7 (Scheme 5) were increased by ~1 to 3° indicating that the C=O and CH_3COO^- groups moved away from the diphenylamine moiety. At the same time, the NH between these two phenyl rings showed a decrease in its angles indicating their simultaneous approach towards each other. This agrees with the fact that as the electronegativity of the substituted metal ion increases, the extent of decrease in these angles increases [18]. At the same time, the C9-C10-Cl12 angle increased in the case of Ca^{2+} and decreased in the Fe^{3+}complex.

The strain in the bond lengths, Table 5, accounting for the change in the nuclear-nuclear repulsions and electron–nuclear attractions was accentuated at the M–O and M–N bonds. Because of the electronegativity values of the cations, the M–O bond lengths are shorter in the complexes than in dic. The coordinate M–N bonds are >2.4A°, and thus unstable. The C6–C5 and C5–C3 bonds in Ca^{2+}, of the acetate group, did not differ much from dic; but in the iron complex were shorter. The C–O bonds were longer in Ca^{2+}than in dic, but shorter in Fe^{3+} (Fig. 3), though its electronegativity is higher than those of the other two. The presence of the d^5 electrons in the ferric ion strains the oxygen slightly away. As for the nitrogen attachment between the phenyl rings, the bonds were longer in both complexes, showing that the drug becomes less stable at this site.

The bond order of these compounds, Table 5, assessed their fragmentation patterns that are depicted in Table 1 The M–O bond for each has the smallest value (0.100 Na^+ and 0.186 $Fe^{3+)}$ except in Ca^{2+}(0.616), where the Ca–N order (0.179) is smaller. The Fe-N order is 0.339.These values are

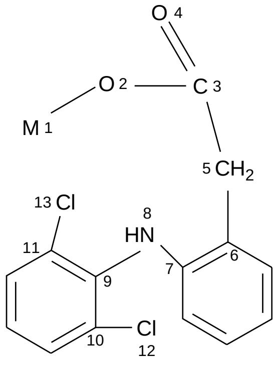

Scheme 5.

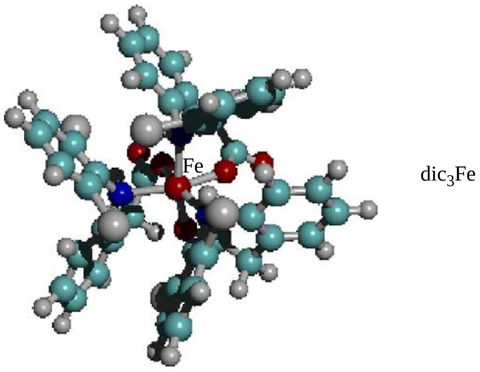

Fig. 3. Optimized structure of Fe^{3+} complex.

in accordance with their very long bond lengths, showing that as in the TG dissociation process, the metals break loose at the very start. In dic, the C6–C5 bond order (0.917) is smaller than that of C5–C3 (0.954); but in the complexes it has a larger value. This explains the dissociation of the acetate moiety as a whole in the sodium salt, while in the complexes the COO^- breaks away first. Though the C-Cl bond order in all three is ∼0.860, the delocalized π-electron cloud of the phenyl ring exerts a mesomeric effect that will result in delayed activity, namely, the stabilization of these bonds [22]. On the other hand, the nitrogen atom, which has bond orders in the range 0.947 to 1.102, is between two phenyl rings. Therefore, it will break its attachments in the same order as the TG fragmentation process.

The dipole moments and energies simulated at the B3LYP/ 6-311G(d) level of theory are depicted in Table 6. The SCF energies of dic, Ca^{2+} and Fe^{3+} decreased as the cation was changed (Na>Ca>Fe). This means that the cation type affects the stability of the drug. This is confirmed by the energy gap values $\Delta E = \text{LUMO} - \text{HOMO}$, that increase in the order $E_{Fe} > E_{Ca} > E_{Na}$. The nuclear-nuclear repulsion energy showed a much higher value (13163.2473au) within the iron complex molecule. These results match the great difference in melting points of the studied compounds.

The magnetic moments, μ, of dic and its complexes clearly assess the above results. The μ of iron was found, using the ZINDO 1 level of theory, to be ∼9 D smaller than that of the calcium complex resulting at the same level of calculation. The direction of μ was always towards the central metal ion; and since Fe^{3+} contains d^5 electrons in its outermost shell, the $\mu_{Ca} > \mu_{Fe}$ is reasonable.

Table 6
Energies, au, and dipole moments, D, of dic and its complexes computed at the 6-311G(d) level

Cation	SCF	LUMO − HOMO	N–N rep. energy	μ
Na^+	−1827.51	5.31E-03	1935.37	11.353
Ca^{2+}	−4007.95	5.89E-03	5729.25	4.275
Fe^{3+}	−6204.86	7.30 (α-orbitals) 7.32 (β-orbitals)	13163.25	ZINDO 1∼8.95[a]

[a] ZINDO 1 gave $\mu_{Ca} = 17.63$ D.

Since μ_{Na} is the largest value, 11.4 D, (Ca being 4.3 D) it is apparent that all the data coincide. The dipole moment values agree with the fact that 100% ionic character possesses the largest μ, decreasing as the character becomes partial. The lone pair on nitrogen gives a very asymmetric distribution of the electronic charge cloud around this atom, producing a large atomic dipole (lone-pair dipole) that opposes the molecule bond dipoles, thus reducing the resultant moment [19].

4. Conclusion

To conclude, the present study that dealt with the mathematical depiction of the energy pyrolysis parameters, as well as, the theoretical assessment of these results, lead to the following points:

1. The activation energies, E*, G*, the activation entropies, S* and the heats of atomization, H*, led to the fact that by replacing the Na^+ by Ca^{2+} or Fe^{3+} the drug became less thermally stable. The results showed that iron manifested catalytic character that increased its k_r and K_s values of its latter loss steps.
2. The thermochemistry of these compounds, that was studied via ab initio calculations at the B3LYP/6-31G(d) level of theory, assessed the experimental results to a quite satisfactory extent.
3. Experimental FT-IR data was used to check the validity of the theoretical calculations. The data were in good agreement.
4. Single point calculations at the B3LYP/6-311G(d) level of theory to compare the geometric parameters, energies and dipole moments of the compounds, assessed the fragmentation loss steps to satisfaction.

Acknowledgements

I would like to extend my deepest gratitude to Prof. Rifaat Hilal for allowing me to have the pleasure of enjoying the work on his *Gaussian 98 W package* of programs. I would also like to thank Mr. Walid M. Ibrahim for his patient guidance during my learning of how to feed in the input.

References

[1] P. Moser, A. Sallmann, I. Wiesenberg, J.Med.Chem. 33 (1990) 2358–2368.
[2] K.M. O'Connor, O.I.Corrigan, Inter. J.Pharm. 226 (1-2) (2001) 163–179.
[3] H. Namazi, M. Babazadeh, A. Sarabi, A. Entezami, J.Poly. Mater. 18 (3) (2001) 301–312.

[4] D. Kovala-Demertzi, D. Mentzafos, A. Terzis, Polyhedron 12 (11) (1993) 1361–1370.
[5] I.M. Kenawi, B.N. Barsoum, M.A. Youssef, Under publication.
[6] A.W. Coats, J.P. Redfern, Nature(London) 68 (1964) 201.
[7] S. Arrhenius, Z.Phys.Chem. 4 (1889) 226; *see:* Trans.Farad.Soc., 33 (1937) 72.
[8] M.J. Frisch, G.W. Trucks, H.B. Schlegel, G.E. Scuseria, M.A. Robb, J.R. Cheeseman, et al., *Gaussian 98, Revision A.6*, Gaussian, Inc., Pittsburgh PA, 1998.
[9] P. Hohenberg, W. Kohn, Phys. Rev. B 136 (1964).
[10] W. Kohn, L.J. Sham, Phys. Rev. A 140 (1965) 1133.
[11] A.D. Becke, Phys. Rev. A 38 (1988) 3098.
[12] C. Lee, W. Yang, R.G. Parr, Phys. Rev.B 37 (1988).
[13] R.L. Flurry Jr, Molecular Orbital Theories of Bonding in Organic Molecules, Marcel Dekker, Inc., New York, 1968.
[14] F.A. Cotton, G. Wilkinson, C.A. Murillo, M. Bochmann,, sixth ed. Advanced Inorganic Chemistry, John Wiley and Sons, Inc., Pte Ltd, Asia, 2003.
[15] I.M. Kenawi, B.N. Barsoum, M.A. Youssef, J. Parm. Biomed Anal. 37 (40), (2005).
[16] A. Fini, M. Garuti, G. Fazio, J. Alvarez-Fuentes, M.A. Holgado, J. Pharm.Sciences 90 (12) (2001) 2049–2057.
[17] L.P. Hammett, Physical Organic Chemistry, McGraw-Hill, Koga-kusha, Ltd, Tokyo, 1970.
[18] L. Pauling, General Chemistry, W.H.Freeman and Co, USA, 1970.
[19] R. Chang, Physical Chemistry for the Chemical and Biological Sciences, University Science Books, USA, 2000.
[20] P. Matthews, Advanced Chemistry, Cambridge Univ. Press, Great Britain, 1997.
[21] J.B. Foresman, A. Frisch,, 2nd ed Exploring Chemistry with Electronic Structural Methods, Gaussian, Inc., Pittsburgh, USA, 1996.
[22] J. March,, fourth ed. Advanced Organic Chemistry: Reactions, Mechanisms, and Structure, John Wiley and Sons, Inc.(Asia), Pte Ltd, Asia, 2000.